Terakawa *Earth, Planets and Space* (2017) 69:87
DOI 10.1186/s40623-017-0671-x

Earth, Planets and Space

FULL PAPER Open Access

# Overpressurized fluids drive microseismic swarm activity around Mt. Ontake volcano, Japan

Toshiko Terakawa*

**Abstract**

Microseismic swarm activity has taken place since 1976 around Mt. Ontake, the second highest stratovolcano in Japan. This activity is thought to be linked to high pore-fluid pressure in the vicinity of the volcano. We analyzed well-constrained focal mechanism solutions of microseismicity to re-estimate the 3-D pore-fluid pressure field driving vigorous swarm activity around Mt. Ontake. Pore-fluid pressures were measured by mapping earthquake focal mechanisms on the 3-D Mohr diagram for the regional stress field with high resolutions of 2–5 km. The assumption of the reference stress pattern can cause modeling errors in measurements of pore-fluid pressure. To remove the effect, we statistically evaluated the estimation errors of the regional stress field and included these errors in the analysis. We detected an overpressurized fluid reservoir with a peak of about 10–30 MPa in the east flank of Mt. Ontake, where microseismic swarm activity has been vigorous for the last two decades. The level of pore-fluid pressure was maintained for at least 5 years after 2009. This finding indicates that there are some interactions between the intensive swarm activity and overpressurized fluids: the swarm activity has been driven by overpressurized fluids, whereas pore-fluid pressures have been suppressed by the swarm activity.

**Keywords:** Pore-fluid pressures, Seismic swarm, Stress field, Earthquake focal mechanisms, Inversion theory

## Introduction

Overpressurized fluids in the Earth's crust are thought to play an important role in earthquake generation (e.g., Nur and Booker 1972; Yamashita 1999; Miller et al. 2004; Sibson 2007). Seismic swarm activity in the vicinity of volcanic regions is widely believed to be controlled by overpressurized fluids (e.g., Ohtake 1974). In the southeast flank of Mt. Ontake, which is the second highest stratovolcano in Japan (Fig. 1), microseismic swarm activity suddenly began to occur in 1976 (Aoki et al. 1980). The vigorous activity has continued for more than four decades since then, and the source region has become enlarged and migrated to the north and east flanks of the mountain (e.g., Ooida et al. 1989; Yamazaki et al. 1992; Rydelek et al. 2002; Terakawa et al. 2013b). During this period, this volcano produced four recorded eruptions (hydrothermal type) with volcanic explosivity index values of 0–2 in 1979, 1991, 2007, and 2014 (e.g., Sawada 1981; Nakamichi et al. 2009; Yamaoka et al. 2016). In 1984, 5 years after the first historic eruption, the western Nagano prefecture earthquake (M 6.8) occurred in the source region of the microseismic swarm (e.g., Ooida et al. 1989; Horiuchi et al. 1992; Yamazaki et al. 1992). The diverse seismicity was suspected to be linked to volcanic eruptions through fluids in the porous network in the underground rock (e.g., Sano et al. 1986), but the relationship among the fluids, diverse seismicity, and eruptions is enigmatic. To date, the presence of fluids has been demonstrated using geophysical, geological, and geochemical methods (e.g., Takahata et al. 2003; Kimata et al. 2004; Kasaya and Oshiman 2004; Yoshimura et al. 2009; Nishio et al. 2010; Doi et al. 2013; Sano et al. 2015), but direct measurement of pore-fluid pressure in the crust is difficult.

An earthquake is a physical process that releases accumulated tectonic stresses by shear faulting, controlled by the Coulomb failure criterion:

*Correspondence: terakawa@seis.nagoya-u.ac.jp
Earthquake and Volcano Research Center, Graduate School of Environmental Studies, Nagoya University, D2-2 (510) Furo-cho, Chikusa-ku, Nagoya 464-8601, Japan

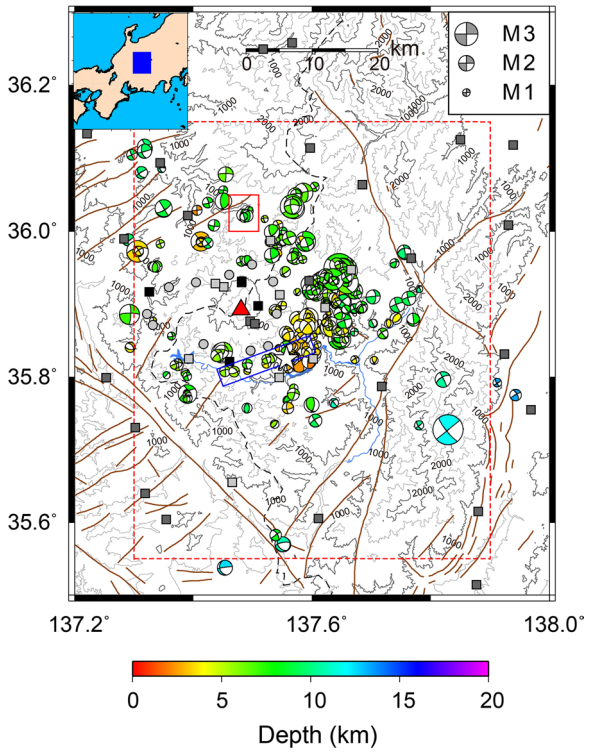


**Fig. 1** Topographic map of Mt. Ontake volcano, seismic stations, and 379 focal mechanisms with $M \geq 1$. Focal mechanism solutions are represented by the lower-hemisphere projection of focal spheres, and the color scale corresponds to focal depth. The *dashed rectangle* in *red* represents the model region in the present FMT analysis. The *red triangle* indicates Mt. Ontake. The *solid circles* and *squares* mark temporary and permanent seismic stations, respectively. The *light gray*, *dark gray*, and *black* symbols denote seismic stations organized by Nagoya University, national institutes (the Japan Meteorological Agency and NIED), and Gifu and Nagano prefectures, respectively. The *white star* and the *blue rectangle* denote the epicenter and the source region of the 1984 Western Nagano prefecture earthquake. The *brown lines* indicate active faults. The *dashed black line* marks the prefectural boundary between Gifu and Nagano prefectures. The *red rectangle* denotes the events that were triggered between June and September, 2011

$$\tau_s = \mu(\sigma_n - P_f) \quad (1)$$

where $\tau_s$ and $\sigma_n$ are the fault (shear) strength and normal stress (positive in compression) on a specified fault, $P_f$ is pore-fluid pressure, and $\mu$ is the intrinsic friction coefficients of rock. When the shear stress reaches the fault strength described by Eq. (1), seismic slip will occur. Seismic slip can be encouraged by both an increase in shear stress and by a decrease in fault strength (Hubbert and Rubey 1959). Therefore, earthquake focal mechanism solutions (fault strike, dip angle, and slip angle) can yield information on the pore-fluid pressure as well as on the stress state in the source region.

Recently, Terakawa et al. (2010) developed an inversion method for estimation of 3-D pore-fluid pressure fields by mapping focal mechanism solutions of seismicity on the 3-D Mohr diagram for a given stress field. In this method, which is termed focal mechanism tomography (FMT) method, the spatial variation in focal mechanisms is attributed to fault strength heterogeneity resulting from spatial variation in pore-fluid pressure. Application of the FMT method to seismicity induced by fluid injection experiments in the Basel Enhanced Geothermal System, Switzerland, quantitatively demonstrated the validity of the method (Terakawa et al. 2012; Terakawa 2014). In these applications, the history of the wellhead pressures of the experiments provided constraints on the inversion results. When applying the method to natural earthquakes, however, evaluating the level of pore-fluid pressure is more difficult.

For the FMT method, it is necessary to know the appropriate stress field and to possess a high-quality dataset of focal mechanism solutions to estimate pore-fluid pressure fields correctly. Terakawa et al. (2013b) applied the FMT method to well-constrained focal mechanism solutions for microseismic swarm activity on the flanks of Mt. Ontake based on the 3-D tectonic stress field over the whole of Japan (longitude: 125°–150°, latitude: 25°–50°, depth: 0–100 km). That study demonstrated that there are overpressurized fluid reservoirs with a peak pressure of more than 100 MPa at depths between 5 and 12 km in the source region of the intensive swarm activity. In the FMT analysis, the spatial variation of the tectonic stress field was taken into account. The tectonic stress field was inferred from 12,500 centroid moment tensor (CMT) data for seismicity ($M > 3.5$) listed in a uniform catalog based on a Japanese nationwide broadband seismograph network organized by the National Research Institute for Earth Science and Disaster Resilience (NIED) by Terakawa and Matsu'ura (2010). The resolution of the tectonic stress pattern expected from the data distribution was an average of 10–20 km horizontally and 5 km vertically. These length scales may not be sufficiently small to estimate the pore-fluid pressures in a limited local region.

Recently, Terakawa et al. (2016) estimated the 3-D regional stress field around Mt. Ontake (longitude: 137.3°–137.9°, latitude: 35.55°–36.15°, depth: 0–20 km) from earthquake focal mechanism solutions obtained through dense seismic networks that monitor microseismicity around Mt. Ontake. The average resolution of the stress pattern was 2–5 km. Using the higher-resolution results for the regional stress field, in the present study, we apply the FMT method to the same dataset as Terakawa et al. (2013b) to re-estimate and re-evaluate the 3-D pore-fluid pressure field around Mt. Ontake. Comparing the pore-fluid pressure fields in the present study with those obtained in Terakawa et al. (2013b), we examine the effects of the assumed stress patterns on estimates of pore-fluid pressures. In addition, we obtain realistic

estimates of the pore-fluid pressures that drive microseismic swarm activity around Mt. Ontake, taking into account the estimation errors of the stress pattern.

## The FMT method

Earthquakes occur on pre-existing faults, governed by the Coulomb failure criterion (Eq. 1). Therefore, variation in earthquake focal mechanisms can be expected even in a uniform stress field (McKenzie 1969). Two end-member models have been proposed to explain the variation in focal mechanisms. One model attributes the variation to differences in the frictional coefficients of rocks, assuming that the pore-fluid pressure field is uniform everywhere; the other model assumes variation in the pore-fluid pressure field with a constant friction coefficient (e.g., Zoback 1992; Rivera and Kanamori 2002). From experimental results and field observations, the intrinsic friction coefficients of rocks are constant at approximately 0.6 at seismogenic depths (e.g., Byerlee 1978; Zoback and Healy 1992; Zoback and Townend 2001), and so we assume the latter model in the FMT method.

The basic assumption of the FMT approach is that seismic slip occurs in the direction of the resolved shear traction acting on the fault (Wallace 1951; Bott 1959), controlled by the Coulomb failure criterion (with a constant intrinsic friction coefficient of rock). Given a stress pattern (normalized deviatoric stress tensor) and using this assumption, it is possible to map a focal mechanism solution on the 3-D Mohr diagram by examining the normal and shear stresses (normalized to the maximum shear stress) acting on the fault plane. This process constrains the relative magnitude of the pore-fluid pressure, because the Coulomb failure criterion is represented by a straight line with a fixed slope (friction coefficient) passing through the point designated by the focal mechanism solution in the Mohr diagram, and the intercept of the line at the horizontal axis yields the (relative) pore-fluid pressure that triggers the event. The absolute pore-fluid pressure can be obtained by further assuming that the vertical stress is the weight of the overburden and that optimally oriented faults relative to the stress pattern are critically stressed under hydrostatic pressure. In addition to the stress pattern with four degrees of freedom, which is usually obtained through stress inversion, these two assumptions are used to determine an absolute stress tensor with six degrees of freedom and the (absolute) pore-fluid pressure. The results for pore-fluid pressures represent the measurements of pore-fluid pressure, $p_n\,(n = 1, \ldots, N)$, at discrete points of the hypocenters $\mathbf{x}_n\,(n = 1, \ldots, N)$.

To discretize the problem, the 3-D excess (above hydrostatic) pore-fluid pressure field is represented by the superposition of the tri-cubic B splines (the basis function), and the expansion coefficients are the model parameters to be solved for the system of linear observation equations. Applying the inversion technique developed by Yabuki and Matsuura (1992) to the excess pore-fluid pressures of the dataset, a static image of the 3-D excess pore-fluid pressure fields can be estimated as a continuous function defined in the mode region with estimation errors (e.g., Terakawa et al. 2012).

## FMT analysis around Mt. Ontake

In this section, we investigated the dependence of pore-fluid pressures on the assumed stress pattern and re-evaluated the 3-D pore-fluid pressure field around Mt. Ontake. We applied the same (FMT) method to the same dataset of earthquake focal mechanism solutions as Terakawa et al. (2013b). We assumed the regional stress field inferred from microseismicity around Mt. Ontake (Terakawa et al. 2016), whereas the stress field used by Terakawa et al. (2013b) was based on part of the tectonic stress field in and around Japan (Terakawa and Matsu'ura 2010). In "Data for the FMT analysis" section, we summarized the dataset to estimate pore-fluid pressure. In "Pore-fluid pressure field with the regional stress pattern" section, we estimated the 3-D distribution of pore-fluid pressure around Mt. Ontake and compared the result with that of Terakawa et al. (2013b). In "Tectonic and regional stress fields around Mt. Ontake" section, we examined the difference between the assumed stress field in the present study and that in the study by Terakawa et al. (2013b). Then, we investigated the effects of the assumed stress field on the results for pore-fluid pressure.

### Data for the FMT analysis

The original dataset for the FMT analysis consists of 993 earthquake focal mechanism solutions ($M \geq -1$) obtained through temporary seismic observations during the summers of 2009–2011 (observation periods: 01/08/2009–05/11/2009, 01/06/2010–09/11/2010, and 15/06/2011–09/11/2011) and permanent seismic observations during the period May 2012 to August 2012. These focal mechanism solutions were estimated using the HASH software package (Hardebeck and Shearer 2002). The uncertainties of the focal mechanism solutions, measured by the root-mean-square angular difference between the best and acceptable focal mechanism solutions, were $\leq 25^\circ$ for 171 events and $\leq 35^\circ$ for 822 events. For the two nodal planes of each focal mechanism solution, we evaluated the misfit angles between the observed slip vector and the shear traction vector (the theoretical slip vector) expected from the regional stress pattern (Terakawa et al. 2016) at the hypocenter. We chose the nodal plane with the smaller misfit angle as the true fault plane. Of 379 focal mechanism solutions with

$M \geq 1$, we used 283 focal mechanism solutions with misfit angles $\leq 25°$ as the final dataset for the FMT analysis.

### Pore-fluid pressure field with the regional stress pattern

The conditions for the FMT analysis were the same as those in Terakawa et al. (2013b) except for the assumed stress field. We targeted the same region around Mt. Ontake (longitude: 137.3°–137.9°, latitude: 35.55°–36.15°, depth: 0–15 km) as the model region for estimating the 3-D pore-fluid pressure field. The pore-fluid pressure field was represented by the superposition of the 2295 ($17 \times 15 \times 19$) tri-cubic B splines; the grid intervals of the tri-cubic B splines were 5 and 2.5 km in the horizontal and vertical directions, respectively. Using the regional stress field obtained by Terakawa et al. (2016), a standard friction coefficient of 0.6, and a rock density value of $2.7 \times 10^3$ kg/m$^3$, we applied the FMT method to the final dataset of focal mechanism solutions ("Data for the FMT analysis" section).

Figure 2a, b shows the pore-fluid pressure field and the estimation errors (the 67% confidence region) at a depth of 5 km; Fig. 2c, d shows the same at 7.5 km depth. For comparison, we illustrate the results obtained in the previous study (Terakawa et al. 2013b) in Additional file 1. In Fig. 3, two profiles of pore-fluid pressures in the present study and those in the study by Terakawa et al. (2013b) along the same latitudes (36.05°, 35.95°, and 35.85°) at depths of 5 and 7.5 km are compared. At latitude 36.05°, both the pore-fluid pressures were consistent within estimation error (Fig. 3a, b). At latitudes 35.95° and 35.85°, the pore-fluid pressures in the shallower part were also generally consistent (Fig. 3c, e); however, there were significant differences between the two profiles at deeper depths (Fig. 3d, f). The pore-fluid pressures in the present study were smaller than those in the study by Terakawa et al. (2013b), with a difference of as much as 110 MPa.

However, the relationship between the event magnitude and the degree of overpressures (Additional file 2) showed a similar tendency to that obtained in the study by Terakawa et al. (2013b). The degree of overpressuring is defined by the overpressure coefficient, $C = (P_f - P_h)/(\sigma_3 - P_h)$, where $P_h$ is hydrostatic pressure and $\sigma_3$ is the minimum compressive principal stress (Terakawa et al. 2012, 2013b). About 40% of small events with $M < 3$ were triggered by overpressurized fluids with $C > 0.3$. In contrast, 90% of the largest ten events ($M \geq 3$) occurred on favorably oriented faults with normalized shear stress >0.5 under near-hydrostatic pressure ($C < 0.3$). From these results, we arrived at the same conclusion as that of Terakawa et al. (2013b) that the larger events were controlled primarily by the tectonic stress rather than by overpressurized fluids.

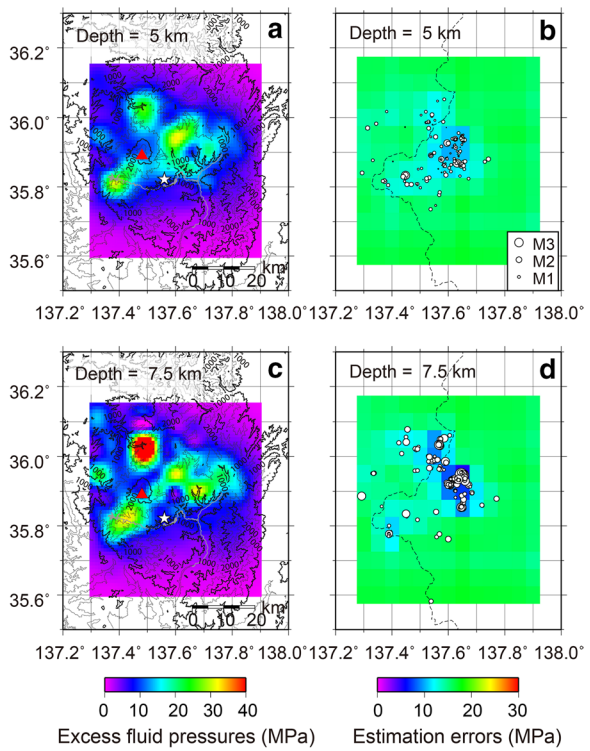


**Fig. 2** The 3-D pore-fluid pressure field around Mt. Ontake. **a** Pore-fluid pressures at a depth of 5 km. **b** Estimation errors of pore-fluid pressures at a depth of 5 km. **c** Pore-fluid pressures at a depth of 7.5 km. **d** Estimation errors of pore-fluid pressures at a depth of 7.5 km. The pore-fluid pressure fields are superposed on the topographic map in (**a**, **c**). The *white circles* in (**b**, **d**) denote the data used in the FMT analysis within 1.25 km from the horizontal plane at 5 and 7.5 km, respectively. The *red triangle* and *white star* are the same as in Fig. 1

### Tectonic and regional stress fields around Mt. Ontake

To examine the effects of the assumed stress pattern on pore-fluid pressures, quantitative comparison of the regional stress field (Terakawa et al. 2016) with the tectonic stress field in and around Japan (Terakawa and Matsu'ura 2010) is necessary. The dataset for the regional stress field consists of 536 earthquake focal mechanism solutions (May 2012 to July 2014, $M \geq 1$) obtained through permanent dense seismic networks that monitor microseismicity in the Ontake region. The dataset for the tectonic stress field consists of 12,500 CMT data for seismicity (January 1997 to January 2007; $M > 3$) listed in the F-net moment tensor catalog, organized by NIED. The latter dataset includes only 22 and 52 events within 30 and 50 km of Mt. Ontake, respectively (Additional file 3), because only 5–10 of more than 3000 events around Mt. Ontake exceed magnitude 3 every year.

The two stress fields were estimated by applying the CMT data inversion method (Terakawa and Matsu'ura

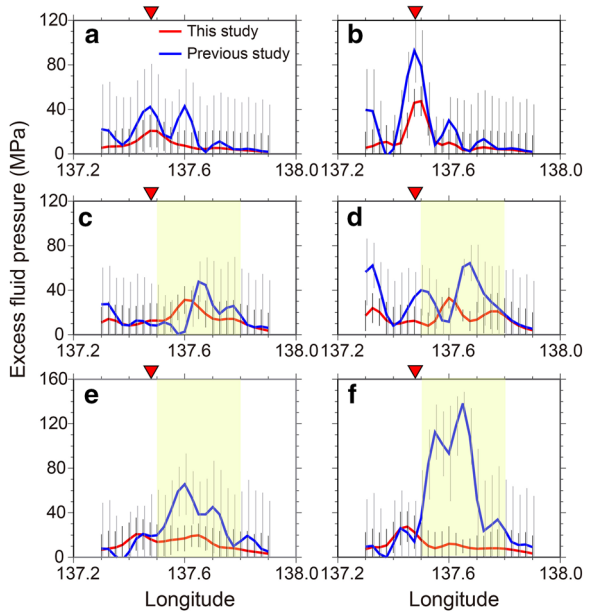


**Fig. 3** Comparison of the latitudinal profiles of pore-fluid pressure fields. The profiles at **a** 36.05° and a depth of 5 km, **b** 36.05° and a depth of 7.5 km, **c** 35.95° and a depth of 5 km, **d** 35.95° and a depth of 7.5 km, **e** 35.85° and a depth of 5 km, and **f** 35.85° and a depth of 7.5 km. The *red* and *blue lines* denote the profiles in the present study and those in the study by Terakawa et al. (2013b), respectively. The *black* and *light gray vertical lines* represent the estimation errors (the 67% confidence region) of pore-fluid pressures in the present study and those in the study by Terakawa et al. (2013b), respectively. The *yellow shaded* zones in (**c**–**f**) correspond to the region A. The *red inverse triangles* denote the longitudinal location of the summit of Mt. Ontake

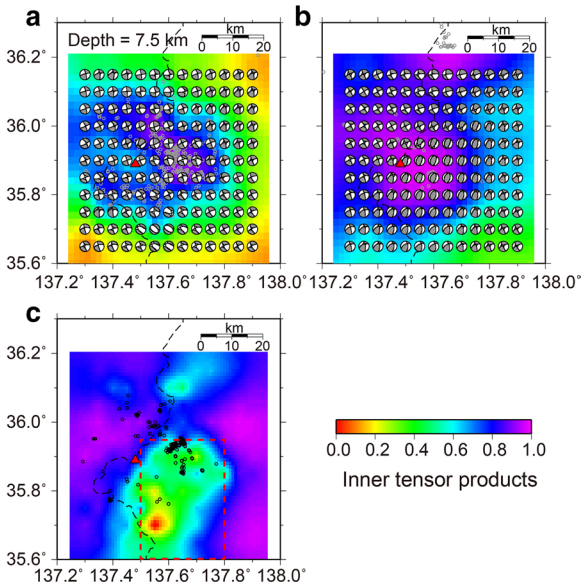


**Fig. 4** Regional and tectonic stress patterns around Mt. Ontake. **a** Regional stress pattern inferred from focal mechanism solutions for May 2012 to July 2014 (Terakawa et al. 2016). **b** Tectonic stress pattern for the Ontake region (Terakawa and Matsu'ura 2010). The *color scales* in **a**, **b** denote the AVITP ("Estimation errors of the regional stress field around Mt. Ontake" section), which was used as the estimation error of the stress field. The *gray open circles* in **a**, **b** indicate the data that were used to infer the regional and tectonic stress fields, respectively. **c** Closeness of the regional and tectonic stress patterns measured with the inner tensor product between the two tensors. The *black open circles* denote the data used to estimate the pore-fluid pressures in "FMT analysis around Mt. Ontake" section. The *dashed rectangle* in *red* represents the region A, where the two stress patterns in **a**, **b** significantly differed

2008) to each dataset. Six components of a stress tensor were represented by the superposition of the tri-cubic B splines. The grid intervals of the tri-cubic B splines for the regional stress field (Terakawa et al. 2016) were 5 and 2.5 km horizontally and vertically, respectively. The number of model parameters for six stress components (the expansion coefficients of the basis functions) was $6 \times 2475$. The grid intervals of the basis function for the tectonic stress field in the whole Japan region (Terakawa and Matsu'ura 2010) were 20 and 10 km horizontally and vertically, respectively. The total number of model parameters was $6 \times 146{,}848$.

Figure 4a shows the regional stress field at high resolution; Fig. 4b shows the tectonic stress field specifically for the Ontake region. In the two stress fields, the axes of maximum compressive principal stresses were commonly in the northwest–southeast direction throughout the whole region, although the results in each figure were based on quite different datasets. In Fig. 4c and Additional file 4, we examined the closeness of the two stress tensors with the inner tensor products (Michael 1987). The quantity ranges from $-1$ to $+1$, where $+1$ indicates that the two stress tensors are exactly the same and $-1$ indicates that they are exactly opposite. Both the stress patterns were characterized by strike-slip faulting with northwest–southeast compression in the whole region (with inner tensor products > 0.8) except for those in the east to south flanks of Mt. Ontake (the region A, longitude: 137.5°–137.8°, latitude: 35.6°–35.95°). The regional stress pattern in the region A was strike-slip type with northwest–southeast compression (Fig. 4a), whereas the tectonic stress pattern was reverse-type with northwest–southeast compression (Fig. 4b). In the region A, the inner tensor products had a mean value of 0.56 (Fig. 4c). This difference in the assumed stress patterns resulted in significant discrepancy in the pore-fluid pressure fields in the region A (Figs. 2, 3). The high-resolution regional stress pattern is more appropriate for estimating pore-fluid pressure fields from microseismicity.

## Pore-fluid pressure drives microseismic swarm activity

Estimation of pore-fluid pressures depends on the assumed stress pattern, as demonstrated in the previous section. The discrepancy between the assumed and true stress patterns yields modeling errors in the estimation of pore-fluid pressure. Unlike random observation errors, modeling errors will cause biased results in inversion analysis (e.g., Yagi and Fukahata 2008). In this section, we consider the estimation errors of the regional stress pattern (Terakawa et al. 2016) in the FMT analysis. In "Estimation errors of the regional stress field around Mt. Ontake" section, we evaluated the estimation errors of the regional stress pattern using multivariate normal random numbers. In "FMT analysis considering estimation errors of the assumed stress pattern" section, we determined the average value of the pore-fluid pressure triggering each event in the final dataset in "Data for the FMT analysis" section, considering the estimation errors of the assumed stress pattern. Subsequently, we applied the FMT method to these data to estimate the pore-fluid pressure field. Comparing the pore-fluid pressure field in "Pore-fluid pressure field with the regional stress pattern" section with that in "FMT analysis considering estimation errors of the assumed stress pattern" section, we evaluated the level of pore-fluid pressure driving microseismic swarm activity.

### Estimation errors of the regional stress field around Mt. Ontake

The CMT data inversion can yield the best estimates and the variance–covariance matrix of the model parameters for the stress field (Terakawa and Matsu'ura 2008). By varying the synthetic model parameters using multivariate normal random numbers with the best estimates of the model parameters (the means) and the variance–covariance matrix, we repeatedly calculated the possible stress patterns for 100 sets. For each set, we measured the closeness between the stress pattern with the best estimates of the model parameters and the pattern with synthetic model parameters using the inner tensor product, and calculated the average value of the inner tensor products of the 100 sets (AVITP) together with the standard deviation (SDVITP). We used the AVITP and the SDVITP as the estimation error of the regional stress pattern and the 67% confidence region, respectively. The AVITP and SDVITP values were larger (the estimation errors were smaller) and smaller, respectively, in the region with more data (Fig. 4a; Additional file 4), which means that the quantities of AVITP and SDVITP are appropriate for estimation errors of the stress pattern and the confidence region, respectively.

### FMT analysis considering estimation errors of the assumed stress pattern

To take the estimation errors of the assumed stress pattern into the FMT analysis, we calculated the pore-fluid pressure triggering the events in the final dataset with the 100 pairs of the synthetic model parameters for the regional stress pattern in "Estimation errors of the regional stress field around Mt. Ontake" section. Subsequently, we determined the average value of the pore-fluid pressure triggering each event. We applied the method in "Pore-fluid pressure field with the regional stress pattern" section to these data to consider the estimation errors of the stress field in this simplified manner, and estimated the pore-fluid pressure field.

Figure 5 shows the profiles of the pore-fluid pressure fields of "Pore-fluid pressure field with the regional stress pattern" section and the profiles of those of this section with the 67% confidence regions along parallel latitudes at 36.05°, 35.95°, and 35.85°. Both the results were consistent within estimation errors. In Figs. 2 and 5, overpressurized fluid reservoirs are visible in the north flank of Mt. Ontake (the region B1, longitude: 137.45°–137.55°,

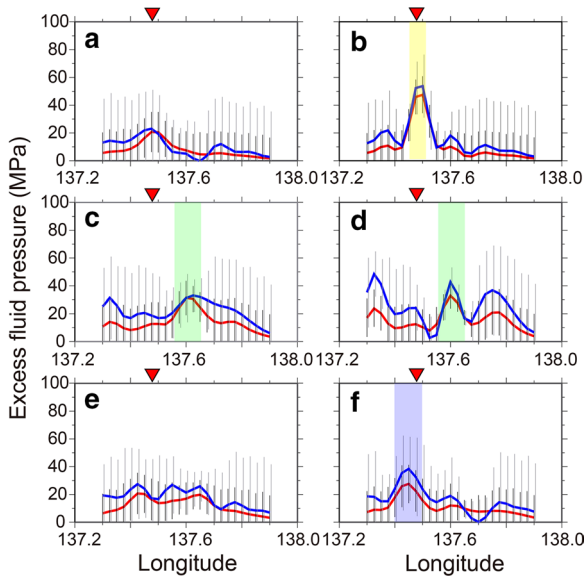


**Fig. 5** FMT analysis considering the estimation errors of the stress fields. The profiles in (**a**–**f**) are displayed in the same way as in Fig. 3. The *red* and *blue lines* denote the pore-fluid pressures that did not and did incorporate the estimation errors of the stress field (in "FMT analysis around Mt. Ontake" and "Pore-fluid pressure drives microseismic swarm activity" sections), respectively. The *black* and *light gray vertical lines* represent the estimation errors (the 67% confidence region) for the analysis in "FMT analysis around Mt. Ontake" and "Pore-fluid pressure drives microseismic swarm activity" sections, respectively. The *yellow*, *green*, and *blue shaded zones* denote the region B1, B2, and B3, respectively. The *red inverse triangles* are the same as those in Fig. 3

latitude: 36.0°–36.1°, depth: 7.5 km), in the east flank of the mountain (the region B2, longitude: 137.55°–137.65°, latitude: 35.85°–35.95°, depth: 5–7.5 km), and in the south flank of the mountain (the region B3, longitude: 137.4°–137.5°, latitude: 35.75°–35.85°, depth: 7.5 km). Pore-fluid pressures in the region B1 have a peak value of 50 ± 20 MPa; those in the region B2, where microseismicity has been most active for more than 20 years, have a peak value of 30 ± 10 MPa. The existence of the two overpressurized fluid reservoirs is reliable within the 95% confidence region. The overpressurized fluid reservoir in the region B3, which is located at the western end of the source region of the 1984 Western Nagano prefecture earthquake, has a peak value of 35 ± 20 MPa (Fig. 5f); however, the existence of the reservoir appears to be uncertain within the 95% confidence region.

## Discussion

We re-evaluated the 3-D pore-fluid pressure field around Mt. Ontake from the same dataset of earthquake focal mechanism solutions used in Terakawa et al. (2013b), but used the high-resolution regional stress field (Terakawa et al. 2016). In the FMT method, we measure pore-fluid pressures by examining fault orientations relative to the stress pattern at hypocenters. When the assumed stress pattern is inappropriate, the modeling errors will yield biased results for pore-fluid pressure. We detected large differences between the two pore-fluid pressure fields in the region A, whose northern part has the most intense microseismic swarm activity for two decades (Figs. 1, 2, 3). Most focal mechanism solutions of the microseismicity were of strike-slip type with P axes along the northwest–southeast direction; these events were generally slip on faults that are favorably oriented to the regional stress pattern (Figs. 1, 4a). However, the tectonic stress pattern, which is the assumed stress pattern of Terakawa et al. (2013b), in the region A was characterized by reverse faulting with northwest–southeast compression (Fig. 4b): these events were slip on misoriented faults to the tectonic stress pattern. In general, there is a larger difference between the shear stresses and fault strength on misoriented faults than that on favorably oriented faults. Therefore, decreases in fault strength resulting from increases in pore-fluid pressure are necessary to trigger events on misoriented faults (Hubbert and Rubey 1959; Hill and Thatcher 1992; Hill 1993). The difference between the assumed stress patterns resulted in that the pore-fluid pressures in the study by Terakawa et al. (2013b) were much larger than those in the present study.

A large discrepancy between the tectonic and regional stress patterns was detected in the region A (Fig. 4c). To investigate whether this difference was significant, we examined the estimation errors of the tectonic stress field in the same way as in "Estimation errors of the regional stress field around Mt. Ontake" section (Fig. 4b). The distribution of the AVITP was relatively uniform, reflecting the rough resolutions of approximately 20 km. Marked spatial changes in AVITP for the regional stress pattern were obvious (Fig. 4a). When the inner tensor product of the two stress tensors is within the 67% confidence regions of the stress pattern, the discrepancy is not significant; otherwise, the difference is not negligible. Quantitative examination (Fig. 4; Additional file 4) revealed that there was a pronounced difference between the two stress patterns in the most part of the region A (longitude: 137.5°–137.5°, latitude: 35.85°–35.95°, depth: 5–7.5 km).

The difference in the stress patterns was directly attributed to the datasets used in the two analyses of stress inversion. The early dataset consists of small to medium events ($M > 3$) for approximately 10 years (Terakawa and Matsu'ura 2010); the later one contains micro to small events ($M \geq 1$) for approximately 2 years (Terakawa et al. 2016). Based on the earthquake scaling laws, the recurrence time for an event with $M = 3$ is expected to be 10 times as long as that for an event with $M = 1$ in a fixed tectonic setting. Thus, if the early data period were 20 years, the two stress patterns would be more similar to each other. In fact, the latest F-net catalog (Jan. 1997 to Feb. 2017) includes strike-slip events in the swarm region (Additional file 3). The relationship between stress and pore-fluid pressure (Additional file 2) indicates that events with relatively large magnitudes are mainly controlled by tectonic processes. In contrast, the microseismic swarm activity is a local phenomenon in a limited region and can be controlled by regional processes rather than large-scale tectonic processes such as plate motion.

Through a series of FMT analyses ("FMT analysis around Mt. Ontake" and "Pore-fluid pressure drives microseismic swarm activity" sections), we detected overpressurized fluid reservoirs in the north and east flanks of Mt. Ontake (the regions B1 and B2) from the seismic data during the period from August 2009 to August 2012. To examine temporal changes in pore-fluid pressure, we applied the method described in "Pore-fluid pressure field with the regional stress pattern" section to another dataset of earthquake focal mechanism solutions. Volcanic earthquake activity related to the 2014 eruption of Mt. Ontake began at the end of August 2014. To remove those effects, we used the data from September 2012 to July 2014. The data were part of the dataset for the regional stress pattern of Terakawa et al. (2016). Except for the deeper part of the region B1, both the pore-fluid pressure fields were basically consistent with each other within the 67% confidence region even though the data periods were completely different (Fig. 6). Overpressurized fluid reservoirs with a peak value of 20 ± 10 MPa were visible at 7.5 km depth in the

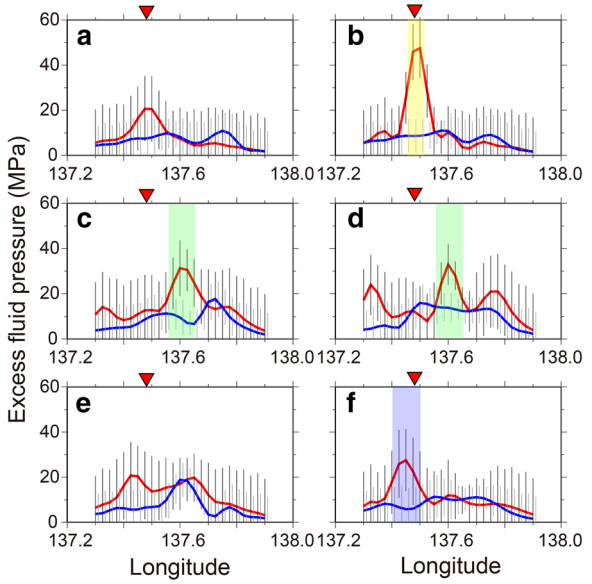


**Fig. 6** Stationarity of the pore-fluid pressure field. The profiles and *vertical lines* in **a**–**f** are displayed in the same way as in Fig. 3. The *red* and *blue lines* denote the pore-fluid pressures estimated from the dataset from June 2009 to August 2012 ("FMT analysis around Mt. Ontake" section) and that from September 2012 to July 2014, respectively. The *color shaded zones* and *red inverse triangles* are the same as those in Fig. 5

region B2 in the results from the new dataset. This finding indicates that the overpressurized fluid reservoirs in the region B2 have maintained a relatively stable state since 2009, suggesting that deep-seated fluids have continuously or intermittently moved into the shallow crust during that period. The fluid supply may have caused the long-term duration of the microseismic swarm activity in that area; on the other hand, the swarm activity may have played a role in the lack of increase in pore-fluid pressure with time.

However, non-negligible temporal changes in pore-fluid pressure were apparent in the region B1. The pore-fluid pressure in the new data period was about 40 $\pm$ 20 MPa lower than that in the original data period (Fig. 6). Going back to the original data (for the periods 01/08/2009–05/11/2009, 01/06/2010–09/11/2010, 15/06/2011–09/11/2011, and 01/05/2012–31/08/2012), we detected eight events with $M \geq 1$ concentrated in the region over a scale of several kilometers (which is included in the region B1) in a relatively short period (Fig. 1). All but one of these events occurred between June and September of 2011, which is just after the off the Pacific coast of Tohoku earthquake ($M_w$ 9.0) in March 2011, although the first three months following the earthquake were not included in the study period. Six of the seven events had reverse-type focal mechanism solutions with northwest–southeast compression, which can be generally explained as reactivation of misoriented pre-existing faults under the regional stress pattern. Unlike the static stress changes, the strong oscillation caused by the mainshock rupture can remotely trigger slip on misoriented faults by elevating fluids confined within the fault zone, and/or by breaking fluid seals at the misoriented faults (Byerlee 1992; Rice 1992; Hill and Thatcher 1992; Hill 1993; Hill et al. 1993; Sibson 2007; Terakawa et al. 2013a). This finding suggests that the 2011 off the Pacific coast of Tohoku earthquake would have enhanced the pore-fluid pressure confined within the misoriented fault zones and triggered the events in the region B1.

The presence of overpressurized fluids in the region B2 is consistent with the ground uplift (2002–2004) caused by a pressure-sourced volume increase that was observed in a precise leveling survey (Kimata et al. 2004). Magneto-telluric measurements demonstrated a low-resistivity zone at depths of 1–5 km in the region B2, which indicates the existence of fluids in that area (e.g., Kasaya et al. 2002; Kasaya and Oshiman 2004; Yoshimura et al. 2009). Nishio et al. (2010) investigated the nature of deep-seated fluids in the Ontake region from groundwater samples (in 2000, 2003, 2005, 2007, and 2009) using lithium and strontium isotopic tools. Moreover, they concluded that the swarm activity in the east flank of Mt. Ontake, which almost corresponds to the region B2, is attributable to non-volcanic fluids in the lower crust. On the other hand, Sano et al. (2015) described constant increases in helium-3 in the east flank of Mt. Ontake (at a site in the region B2) for more than 20 years prior to the 2014 eruption, implying that volcanic fluids beneath Mt. Ontake were involved in driving the swarm activity. The sites of fluid sources revealed by previous studies are mainly located in the western part of the overpressurized fluid reservoirs in the region B2. Most previous studies involved an investigation designed to elucidate the relationship between fluids and the 1984 Western Nagano prefecture earthquake, which may have caused the small shift of the fluid sources to the west from the center of the region B2. Nevertheless, there may be an upwelling system of mantle fluids beneath the central cone of Mt. Ontake and/or non-volcanic deep-seated fluids in the lower crust to the east flank (Nishio et al. 2010; Sano et al. 2015).

Finally, the relationship of pore-fluid pressure to the phreatic eruptions of Mt. Ontake is of great interest. Theoretically, pore-fluid pressure can be estimated beneath the volcano from focal mechanism solutions of volcano-tectonic (VT) events in the same way. However, the VT events beneath Mt. Ontake are very small ($M < 1$), and obtaining reliable focal mechanism solutions is more complicated. Unfortunately, data for VT events are not included in the present study. In addition, the local stress field beneath the summit may change with the volcanic activity (Terakawa et al. 2016). Information on stress fields is important for estimating pore-fluid pressure, and so it is necessary to

estimate the temporal stress changes beneath the summit correctly. Terakawa et al. (2016) also demonstrated slight deviation of the focal mechanisms of swarm activity from the typical type in the east flank (longitude: 137.6°–137.7°, latitude: 35.85°–35.95°) for a week before the 2014 eruption. It is interesting to reveal the below-ground porous network and to understand how overpressurized fluids may link volcanic activity and diverse seismicity around the volcano.

## Conclusions

We re-estimated the 3-D pore-fluid pressure field around Mt. Ontake from earthquake focal mechanism solutions for a long period of time (June 2009 to July 2014), based on the regional stress field with a high resolution of 2–5 km. The choice of reference stress pattern can cause systematic modeling errors; therefore, we statistically evaluated the estimation errors of the regional stress field and incorporated them into the FMT analysis in a simplified manner. These examinations yielded the conclusion that the microseismic swarm activity in the east flank of Mt. Ontake has been driven by pore-fluid pressures of about 10–30 MPa.

## Additional files

**Additional file 1.** The 3-D pore-fluid pressure field around Mt. Ontake estimated in Terakawa et al. (2013b). (a) Pore-fluid pressures at a depth of 5 km. (b) Estimation errors of pore-fluid pressures at a death of 5 km. (c) Pore-fluid pressures at a depth of 7.5 km. (d) Estimation errors of pore-fluid pressures at a death of 7.5 km. The pore-fluid pressure fields are superposed on the topographic map in (a) and (c). The white circles in (b) and (d) denote the data used in the FMT analysis within 1.25 km from the horizontal plane at 5 and 7.5 km, respectively. The red triangle indicates Mt. Ontake. The white star denotes the epicenter of the 1984 Western Nagano prefecture earthquake.

**Additional file 2.** Roles of pore-fluid pressure and tectonic stress in earthquake generation. (a) Relationship between event magnitudes and pore-fluid pressures activating the events. The vertical axis denotes the overpressure coefficient C (see text). (b) Relationship between event magnitudes and shear stress acting on fault planes. The vertical axis shows shear stress normalized by the maximum shear stress at the hypocentral depth. Open diamonds in (b) denote seismic events triggered by pore-fluid pressures with $C < 0.2$ (near-hydrostatic pressures). Note that we did not use events with $M < 1$ for estimating the 3-D pore-fluid pressure field.

**Additional file 3.** The CMT data of seismicity listed in the F-net seismic moment tensor catalog (Jan. 1997 to Feb. 2017). The CMT data are plotted using a lower-hemisphere stereographic projection of focal spheres. The blue and red focal spheres are data during the period of January 1997 to January 2007 (the first data period), and February 2007 to February 2017, respectively. The CMT data in the first period are included in the dataset to estimate the 3-D tectonic stress field in and around Japan (Terakawa and Matsu'ura 2010).

**Additional file 4.** Difference between the regional and tectonic stress fields. The red lines show the closeness of the two stress tensors measured by the inner tensor product (Michael 1987). The light blue and blue lines denote the estimation errors of the regional and tectonic stress patterns, respectively. The estimation errors of the stress fields are represented with the average value of the inner tensor products of 100 possible stress patterns (AVITP, see text). The black and light gray bars show the standard deviation of the inner tensor products (SDVITP, see text).

### Abbreviations

AVITP: the average value of the inner tensor products; SDVITP: the standard deviation of the inner tensor products.

### Acknowledgements

I would like to thank Yoshiko Yamanaka for discussion, and Shinichiro Horikawa and Takashi Okuda for seismic observations. I thank the editor, Yoshihisa Iio and anonymous reviewers for useful comments and suggestions. I am grateful to Japan Meteorological Agency, National Research Institute for Earth Science and Disaster Prevention (NIED), Nagano and Gifu prefectures for providing seismic waveform data. I would like to thank Enago (www.enago.jp) for the English language review.

### Competing interests

The author declares no competing interests.

### Availability of data and materials

The data that support the findings of this study are available from the corresponding author on request.

### Funding

This work was partially supported by the Earthquake Research Institute cooperative research program and in part by a Grant-in Aid for Scientific Research C (26400451).

## Publisher's Note



Received: 24 March 2017 Accepted: 20 June 2017
Published online: 29 June 2017

### References

Aoki H, Ooida T, Fujii I, Yamazaki F (1980) Seismological study on the 1979 eruption of Ontake volcano. In: Aoki H (ed) Investigation of Volcanic activity and disasters caused by the 1979 eruption of Ontake volcano. The Ministry of Education, Science and Culture of Japan, Tokyo **(in Japanese)**

Bott MHP (1959) The mechanics of oblique slip faulting. Geol Mag 96:109–117

Byerlee J (1978) Friction of rocks. Pure appl Geophys 116:615–626

Byerlee J (1992) The change in orientation of subsidiary shears near faults containing pore fluid under high-pressure. Tectonophysics 211:295–303

Doi I, Noda S, Iio Y, Horiuchi S, Sekiguchi S (2013) Relationship between hypocentral distributions and Vp/Vs ratio structures inferred from dense seismic array data: a case study of the 1984 western Nagano Prefecture earthquake, central Japan. Geophys J Int 195:1323–1336

Hardebeck JL, Shearer PM (2002) A new method for determining first-motion focal mechanisms. Bull Seismol Soc Am 92:2264–2276

Hill DP (1993) A note on ambient pore pressure, fault-confined pore pressure, and apparent friction. Bull Seismol Soc Am 83:583–586

Hill DP, Thatcher W (1992) An energy constraint for frictional slip on misoriented faults. Bull Seismol Soc Am 82:883–897

Hill DP, Reasenberg PA, Michael A, Arabaz WJ, Beroza G, Brumbaugh D, Brune JN, Castro R, Davis S, Depolo D, Ellsworth WL, Gomberg J, Harmsen S, House L, Jackson SM, Johnston MJS, Jones L, Keller R, Malone S, Munguia L, Nava S, Pechmann JC, Sanford A, Simpson RW, Smith RB, Stark M, Stickney M, Vidal A, Walter S, Wong V, Zollweg J (1993) Seismicity remotely triggered by the magnitude 7.3 Landers, California, earthquake. Science 260:1617–1623

Horiuchi S, Ito K, Moriya T, Nishigami K, Ooida T, Ouchi T, Tanada T, Tsukuda T, Yamazaki F, Aoki H, Fujii I, Haneda T, Hasegawa A, Hashimoto S, Hirahara K, Hirata N, Hirano N, Iio Y, Ikami A, Ishiketa Y, Ito A, Kanazawa T, Kaneshima S, Karakama I, Kobayashi M, Koizumi M, Kono T, Kosuga M, Kurata Y, Kuriyama S, Kuroiso A, Matsuzawa T, Mikumo T, Mitsunami T, Miura K, Miyajima R, Miyamachi H, Mizoue M, Nakajima A, Nakamura I, Nakamura M, Nakayama T, Oike K, Okamoto T, Ohkura T, Saeki T, Sakai K, Shibutani T, Suzuki M, Suzuki S, Takahashi M, Takagi A, Takeuchi F, Tomita S, Umeda Y, Wada H, Yabuki T, Yamada M, Yamamoto A, Yamashina K, Yokohama M (1992) Hypocenter locations by a dense network. J Phys Earth 40:313–326

Hubbert MK, Rubey WW (1959) Role of fluid pressure in mechanics of overthrust faulting 1. Mechanics of fluid-filled porous solids and its application to overthrust faulting. Geol Soc Am Bull 70:115–166
Kasaya T, Oshiman N (2004) Lateral inhomogeneity deduced from 3-D magnetotelluric modeling around the hypocentral area of the 1984 Western Nagano Prefecture earthquake, central Japan. Earth Planets Space 56:547–552
Kasaya T, Oshiman N, Sumitomo N, Uyeshima M, Iio Y, Uehara D (2002) Resistivity structure around the hypocentral area of the 1984 Western Nagano Prefecture earthquake in central Japan. Earth Planets Space 54:107–118
Kimata F, Miyajima R, Murase M, Darwaman D, Ito T, Ohata Y, Irwan M, Takano K, Ibrahim F, Koyama E, Tsuji H, Takayama T, Uchida K, Okada J, Solim D, Anderson H (2004) Ground uplift detected by precise leveling in the Ontake earthquake swarm area, central Japan in 2002–2004. Earth Planets Space 56:E45–E48. doi:10.1186/BF03352514
McKenzie DP (1969) Relation between fault plane solutions for earthquakes and directions of principal stresses. Bull Seismol Soc Am 59:591–601
Michael AJ (1987) Use of focal mechanisms to determine stress—a control study. J Geophys Res Solid Earth Planets 92:357–368
Miller SA, Collettini C, Chiaraluce L, Cocco M, Barchi M, Kaus BJP (2004) Aftershocks driven by a high-pressure $CO_2$ source at depth. Nature 427:724–727
Nakamichi H, Kumagai H, Nakano M, Okubo M, Kimata F, Ito Y, Obara K (2009) Source mechanism of a very-long-period event at Mt Ontake, central Japan: response of a hydrothermal system to magma intrusion beneath the summit. J Volcanol Geotherm Res 187:167–177
Nishio Y, Okamura K, Tanimizu M, Ishikawa T, Sano Y (2010) Lithium and strontium isotopic systematics of waters around Ontake volcano, Japan: implications for deep-seated fluids and earthquake swarms. Earth Planet Sci Lett 297:567–576
Nur A, Booker JR (1972) Aftershocks caused by pore fluid-flow. Science 175:885–887
Ohtake M (1974) Seismic activity induced by water injection at Matsushiro, Japan. J Phys Earth 22:163–176
Ooida T, Yamazaki F, Fujii I, Aoki H (1989) Aftershock activity of the 1984 Western Nagano prefecture earthquake, central Japan, and its relation to earthquake swarms. J Phys Earth 37:401–416
Rice JR (1992) Fault stress states, pore pressure distributions, and the weakness of the San Andreas fault. In: Evance B, Wong TF (eds) Fault mechanics and transport properties of rocks. Academic Press, San Diego, pp 475–503
Rivera L, Kanamori H (2002) Spatial heterogeneity of tectonic stress and friction in the crust. Geophys Res Lett. doi:10.1029/2001GL013803
Rydelek PA, Horiuchi S, Iio Y (2002) Spatial and temporal characteristics of low-magnitude seismicity from a dense array in western Nagano Prefecture, Japan. Earth Planets Space 54:81–89. doi:10.1186/BF03351709
Sano Y, Nakamura Y, Wakita H, Notsu K, Kobayashi Y (1986) $^3HE/^4HE$ ratio anomalies associated with the 1984 Western Nagano earthquake—possibly induced by a diapiric magma. J Geophys Res Solid Earth Planets 91:2291–2295
Sano Y, Kagoshima T, Takahata N, Nishio Y, Roulleau E, Pinti DL, Fischer TP (2015) Ten-year helium anomaly prior to the 2014 Mt Ontake eruption. Sci Rep. doi:10.1038/srep13069
Sawada Y (1981) Ontake volcano. Bull Volcan Erupt 19:49–51
Sibson RH (2007) An episode of fault-valve behaviour during compressional inversion? The 2004 M(J)6.8 Mid-Niigata Prefecture, Japan, earthquake sequence. Earth Planet Sci Lett 257:188–199
Takahata N, Yokochi R, Nishio Y, Sano Y (2003) Volatile element isotope systematics at Ontake volcano, Japan. Geochem J 37:299–310
Terakawa T (2014) Evolution of pore fluid pressures in a stimulated geothermal reservoir inferred from earthquake focal mechanisms. Geophys Res Lett 41:7468–7476
Terakawa T, Matsu'ura M (2008) CMT data inversion using a Bayesian information criterion to estimate seismogenic stress fields. Geophys J Int 172:674–685
Terakawa T, Matsu'ura M (2010) The 3-D tectonic stress fields in and around Japan inverted from centroid moment tensor data of seismic events. Tectonics. doi:10.1029/2009TC002626
Terakawa T, Zoporowski A, Galvan B, Miller SA (2010) High-pressure fluid at hypocentral depths in the L'Aquila region inferred from earthquake focal mechanisms. Geology 38:995–998
Terakawa T, Miller SA, Deichmann N (2012) High fluid pressure and triggered earthquakes in the enhanced geothermal system in Basel, Switzerland. J Geophys Res Solid Earth. doi:10.1029/2011JB008980
Terakawa T, Hashimoto C, Matsu'ura M (2013a) Changes in seismic activity following the 2011 Tohoku-oki earthquake: effects of pore fluid pressure. Earth Planet Sci Lett 365:17–24
Terakawa T, Yamanaka Y, Nakamichi H, Watanabe T, Yamazaki F, Horikawa S, Okuda T (2013b) Effects of pore fluid pressure and tectonic stress on diverse seismic activities around the Mt. Ontake volcano, central Japan. Tectonophysics 608:138–148
Terakawa T, Kato A, Yamanaka Y, Maeda Y, Horikawa S, Matsuhiro K, Okuda T (2016) Monitoring eruption activity using temporal stress changes at Mount Ontake volcano. Nat Commun. doi:10.1038/ncomms10797
Wallace RE (1951) Geometry of shearing stress and relation of faulting. J Geol 59:118–130
Yabuki T, Matsuura M (1992) Geodetic data inversion using a bayesian information criterion for spatial-distribution of fault slip. Geophys J Int 109:363–375
Yagi Y, Fukahata Y (2008) Importance of covariance components in inversion analyses of densely sampled observed data: an application to waveform data inversion for seismic source processes. Geophys J Int 175:215–221
Yamashita T (1999) Pore creation due to fault slip in a fluid-permeated fault zone and its effect on seismicity: generation mechanism of earthquake swarm. Pure appl Geophys 155:625–647
Yamaoka K, Geshi N, Hashimoto T, Ingebritsen SE, Oikawa T (2016) Special issue "The phreatic eruption of Mt. Ontake volcano in 2014". Earth Planets Space 68:175. doi:10.1186/s40623-016-0548-4
Yamazaki F, Horiuchi S, Ito K, Moriya T, Nishigami K, Ooida T, Ouchi T, Tanada T, Tsukuda T, Aoki H, Fujii I, Haneda T, Hasegawa A, Hashimoto S, Hirahara K, Hirano N, Hirata N, Iio Y, Ikami A, Ishiketa Y, Ito A, Kanazawa T, Kaneshima S, Karakama I, Kobayashi M, Koizumi M, Kono T, Kosuga M, Kurata Y, Kuriyama S, Kuroiso A, Matsuzawa T, Mikumo T, Mitsunami T, Miura K, Miyajima R, Miyamachi H, Mizoue M, Nakajima A, Nakamura I, Nakamura M, Nakayama T, Oike K, Okamoto T, Okuda T, Saeki T, Sakai K, Shibutani T, Suzuki M, Suzuki S, Takahashi M, Takagi A, Takeuchi F, Tomita S, Umeda Y, Wada H, Yabuki T, Yamada M, Yamamoto A, Yamashina K, Yokohama M (1992) Focal mechanism analyses of aftershocks of the 1984 Western Nagano prefecture earthquake. J Phys Earth 40:327–341
Yoshimura R, Ohsiman N, Kasaya T, Iio Y, Miura T, Nishimura K, Yamazaki T, Higa T, Hirose N, Taira K (2009) AMT observation around the focal region of the 1984 Western Nagno earthquake. Ann Disas Prev Res Inst Kyoto Univ 52B:249–254
Zoback ML (1992) Stress-field constraints on intraplate seismicity in Eastern North-America. J Geophys Res Solid Earth 97:11761–11782
Zoback MD, Healy JH (1992) In situ stress measurements to 3.5 km depth in the Cajon pass scientific-research borehole—implications for the mechanics of crustal faulting. J Geophys Res Solid Earth 97:5039–5057
Zoback MD, Townend J (2001) Implications of hydrostatic pore pressures and high crustal strength for the deformation of intraplate lithosphere. Tectonophysics 336:19–30